All-Optical Wavelength Preserved Modulation Format Conversion From PDM-QPSK to PDM-BPSK Using FWM and Interference

Hiroki Kishikawa, *Member, IEEE*, Nobuo Goto, *Member, IEEE*, and Lawrence R. Chen, *Senior Member, IEEE*

***Abstract*—Flexible conversion between multi-level modulation formats is one of the key processing functions to realize adaptive modulation techniques for flexible networking aimed at high spectral efficiency in optical fiber transmission. The authors have proposed an all-optical format conversion systems from binary phase-shift keying (BPSK) to quadrature PSK (QPSK) and its reverse conversion from QPSK to BPSK. The latter had an advantage of wavelength-shift-free conversion from an incident QPSK to simultaneous two BPSK outputs without loss of the transmitting data. However, it was limited only for a single polarization signal. In this paper, we propose a novel method of wavelength preserved conversion for polarization division multiplexed QPSK signal with arbitrary polarization rotation angle to the x-axis on the x-y polarization plane which is orthogonal to the propagation axis. The method is based on the orthogonal dual-pump four-wave-mixing (FWM) in the highly nonlinear fiber with a nonlinear optical loop mirror configuration, which has advantages that it separately outputs the original signal and the phase conjugate signal and has independent FWM efficiency of the signal polarization angle. We show the system performances such as bit-error-rate and optical signal-to-noise ratio penalty evaluated by numerical simulations.**

***Index Terms*—Optical processing, modulation format, four-wave mixing, PDM-QPSK, PDM-BPSK**

I. Introduction

ADVANCED modulation formats have been widely exploited as one of the promising technologies to increase transmission capacity and spectral efficiency (SE) in optical fiber communications with developing digital signal processing to meet the demand in growing communication traffic [1], [2]. Flexible conversion between different levels of multi-level modulation formats without optical-to-electrical and electrical-to-optical conversions will be expected to realize adaptive modulation and demodulation technologies and efficient use of the fiber spectral resources for elastic optical networks.

In order to increase SE, various all-optical methods have been studied for conversions from lower-order to higher-order modulation formats. For instance, conversions from on-off-keying (OOK) to binary phase-shift keying (BPSK), quadrature PSK (QPSK), or 8 PSK have been developed by using nonlinear effects in a highly nonlinear fiber (HNLF) and a semiconductor optical amplifier (SOA) [3], [4]. Conversions among different m-ary PSKs, we have proposed a passive interference method to convert from BPSK to QPSK [5], and the same principle was further applied to convert to quadrature amplitude modulation (QAM) [6].

Reverse conversions from higher-order to lower-order modulation formats are suitable when the signals transmitted in long-haul are then redirected to short-reach or local transmission [7]. For instance, several nonlinear methods have been reported for conversions from QPSK to BPSK format. Methods such as using phase erasure by four-wave mixing (FWM) [8], and using phase-sensitive FWM in SOA [7], [9], HNLF [10] or periodically poled lithium niobate (PPLN) [11] have been reported. The method [8] outputs only a half of the original data sequence as a BPSK stream by using a single pump light. The methods [7], [10], [11] create two BPSK tributaries without loss of the original data; however, four phase-arranged pump lights are required. The method [9] extract two BPSK tributaries onto the two orthogonal polarizations by using a pump and four phase-arranged orthogonal probes. The output BPSK signal in these methods has a different wavelength from the incident QPSK signal. Such wavelength difference would be ineffective since it might need additional wavelength conversion when a signal once isolated for format conversion is re-inserted into the same wavelength channel among other WDM channels.

To overcome the issue, some wavelength preserved conversion techniques have been reported so far. The method proposed in [12] uses phase-squeezing by phase sensitive amplification (PSA) in HNLF or PPLN. Experimental demonstration using dual-pump PSA [13] demultipexed each BPSK tributaries from a QPSK signal separately, namely, the in-phase or quadrature component of the input QPSK signal can be selected by adjusting the relative phase. Recently proposed conversion methods [14] and [15] also experimentally extracted two BPSK tributaries by using polarizers and a polarization beam splitter (PBS), respectively. Similar technique has been further applied to decompose a 16QAM signal in [16]. Methods in [14], [17] have reported that both BPSK tributaries can be simultaneously extracted by using a PBS when the parametric gain is sufficiently high so that the original signal and the phase conjugate idler match in intensity. Our previously reported method [18], [19] converted a QPSK signal to two BPSK tributaries simultaneously without loss of the original data by using FWM and interference, in which the quantitative analyses based on bit-error-rate (BER) were performed by numerical simulations. Above methods are

This research was supported in part by JSPS KAKENHI (15H06443).

H. Kishikawa and N. Goto are with the Department of Optical Science, Tokushima University, Tokushima 770-8506, Japan

L. R. Chen is with the Department of Electrical and Computer Engineering at McGill University, Montreal QC H3A 2A7, Canada

(e-mail:kishikawa.hiroki@tokushima-u.ac.jp)

limited to apply only to a single polarization input signal with restricted polarization alignment of signal and pump waves.

To the best of our knowledge, no conversion techniques from polarization division multiplexed (PDM)-QPSK signals to PDM-BPSK signals have been reported so far. Although our previously reported method [20] using a polarization-diversity setup has aimed at polarization-insensitive conversion, it has yet been for a single polarization QPSK signal. In this paper, therefore, we propose a novel method of wavelength preserved conversion for PDM-QPSK signals which can be applied to arbitrary polarization rotation angle to the x-axis on the x-y polarization plane which is orthogonal to the propagation axis. This paper is organized as follows. The concept and the detailed operation principle of the proposed scheme is described in section II. Quantitative analyses based on BER are described in section III so as to assess the conversion system performance such as dependencies of signal OSNR, signal power, pump power, polarization rotation angle, and laser linewidth by numerical simulations. Issues to be considered for practical use of the proposed system are also discussed in section IV. Finally, conclusion and our future works are described in section V.

II. Operation principle

Fig. 1 shows the schematic diagram of the proposed format conversion system and signal spectra at each point. The setup shown in Fig. 1(a) has two basic building blocks, that is, the phase conjugator and the format converter. The phase conjugator consists of a HNLF, a 3-dB coupler, circulators and band-pass filters (BPFs). The principle of generating phase conjugate signal from original signal by using orthogonal dual-pump FWM in the HNLF with a nonlinear optical loop mirror (NOLM) configuration has been reported in [21]. This method has advantages that the original signal and the phase conjugate signal come out at different ports separately and FWM efficiency is independent of the signal polarization angle. In Fig. 1(a), the original signal passes through the upper BPF and is attenuated to have the same intensity as the weaker phase conjugate signal going through the lower BPF.

The format converter located in the latter part of the configuration consists of Y-dividers, Y-combiners, polarization rotators, polarization beam splitters (PBSs) and polarization beam combiners (PBCs). Thanks to the feature of the phase conjugator, the polarization angle of the phase conjugate signal is controlled individually. Then, the original QPSK signal and the phase conjugate QPSK signal are superimposed by the Y-combiners, thereby being converted to two BPSK signals. By using PBSs and PBCs, y-polarization component of the converted BPSK signals are exchanged and reconstructed to in-phase PDM-BPSK and quadrature PDM-BPSK signals.

Here we formulate the conversion operation using the Jones calculus. As shown in Fig. 1(b), an original PDM-QPSK signal is combined with orthogonally polarized two pumps at the 3-dB coupler, and then these signals are incident into the HNLF. The original PDM-QPSK signal in the HNLF is written as

$$\begin{pmatrix} E_{sx} \\ E_{sy} \end{pmatrix} = \begin{pmatrix} E_x \exp(i(\omega_s t - \beta_s z + \phi_x(t))) \\ E_y \exp(i(\omega_s t - \beta_s z + \phi_y(t) + \theta)) \end{pmatrix} \quad (1)$$

where E_x and E_y are the real-valued pulse envelopes, $i = \sqrt{-1}$, $\omega_s = 2\pi f_s$ is the angular frequency, β_s is the propagation constant, $\phi_x(t)$ and $\phi_y(t)$ are the QPSK phases at each polarization component, θ is the time invariant phase difference between x- and y-polarization components. Note that only QPSK phase terms relevant to $\phi_x(t)$ and $\phi_y(t)$ are indicated on schematic signal spectra of each polarization component in Figs. 1(b)-(i) for simplicity. Two continuous wave (CW) pumps are written as

$$\begin{pmatrix} E_{px} \\ E_{py} \end{pmatrix} = \begin{pmatrix} E_{p1} \exp(i(\omega_{p1} t - \beta_{p1} z)) \\ E_{p2} \exp(i(\omega_{p2} t - \beta_{p2} z)) \end{pmatrix} \quad (2)$$

where E_{p1} and E_{p2} are the real-valued amplitudes, $\omega_{p1} = 2\pi f_{p1}$ and $\omega_{p2} = 2\pi f_{p2}$ are the angular frequencies, β_{p1} and β_{p2} are the propagation constants. We assume that angular frequencies are chosen to be $\omega_{p1} + \omega_{p2} = 2\omega_s$ to induce center frequency preserved FWM and the phase matching condition $\beta_{p1} + \beta_{p2} = 2\beta_s$ is satisfied.

The orthogonal dual pump FWM generates a phase conjugate signal at the same center frequency while at the orthogonal side of the polarization compared to the original signal, namely, the x-polarization component of the original signal contributes to produce the y-polarization component of the phase conjugate signal, and vice versa. It is still overlapped with the original signal at the end of the HNLF as shown in Fig. 1(c), however, they are separated after passing back the 3-dB coupler. The separated phase conjugate signal is written as [21]

$$\begin{pmatrix} E_{Fx} \\ E_{Fy} \end{pmatrix} = \begin{pmatrix} \kappa E_y E_{p1} E_{p2} \exp(i(\omega_s t - \beta_s L - \phi_y(t) - \theta)) \\ \kappa E_x E_{p1} E_{p2} \exp(i(\omega_s t - \beta_s L - \phi_x(t))) \end{pmatrix} \quad (3)$$

where κ is the FWM efficiency, L is the HNLF length, and $\exp(-i\phi_x(t))$ and $\exp(-i\phi_y(t))$ correspond to the complex conjugate phase terms. For simplicity, the time-space factor $\exp(i(\omega_s t - \beta_s L))$ is not shown in the following equations.

The phase conjugate signal is divided into two streams and they are polarization rotated at $+90$ and -90 degrees, respectively, as shown in Figs. 1(d) and 1(e). These signals can be calculated as

$$\begin{aligned} \begin{pmatrix} E_{(\mathrm{d})x} \\ E_{(\mathrm{d})y} \end{pmatrix} &= \frac{1}{\sqrt{2}} \begin{pmatrix} \cos(-90) & -\sin(-90) \\ \sin(-90) & \cos(-90) \end{pmatrix} \times \\ &\quad \begin{pmatrix} \alpha E_y \exp(-i(\phi_y(t) + \theta)) \\ \alpha E_x \exp(-i\phi_x(t)) \end{pmatrix} \\ &= \frac{1}{\sqrt{2}} \begin{pmatrix} \alpha E_x \exp(-i\phi_x(t)) \\ -\alpha E_y \exp(-i(\phi_y(t) + \theta)) \end{pmatrix}, \end{aligned} \quad (4)$$

$$\begin{aligned} \begin{pmatrix} E_{(\mathrm{e})x} \\ E_{(\mathrm{e})y} \end{pmatrix} &= \frac{1}{\sqrt{2}} \begin{pmatrix} \cos(90) & -\sin(90) \\ \sin(90) & \cos(90) \end{pmatrix} \times \\ &\quad \begin{pmatrix} \alpha E_y \exp(-i(\phi_y(t) + \theta)) \\ \alpha E_x \exp(-i\phi_x(t)) \end{pmatrix} \\ &= \frac{1}{\sqrt{2}} \begin{pmatrix} -\alpha E_x \exp(-i\phi_x(t)) \\ \alpha E_y \exp(-i(\phi_y(t) + \theta)) \end{pmatrix} \end{aligned} \quad (5)$$

where $\alpha = \kappa E_{p1} E_{p2}$.

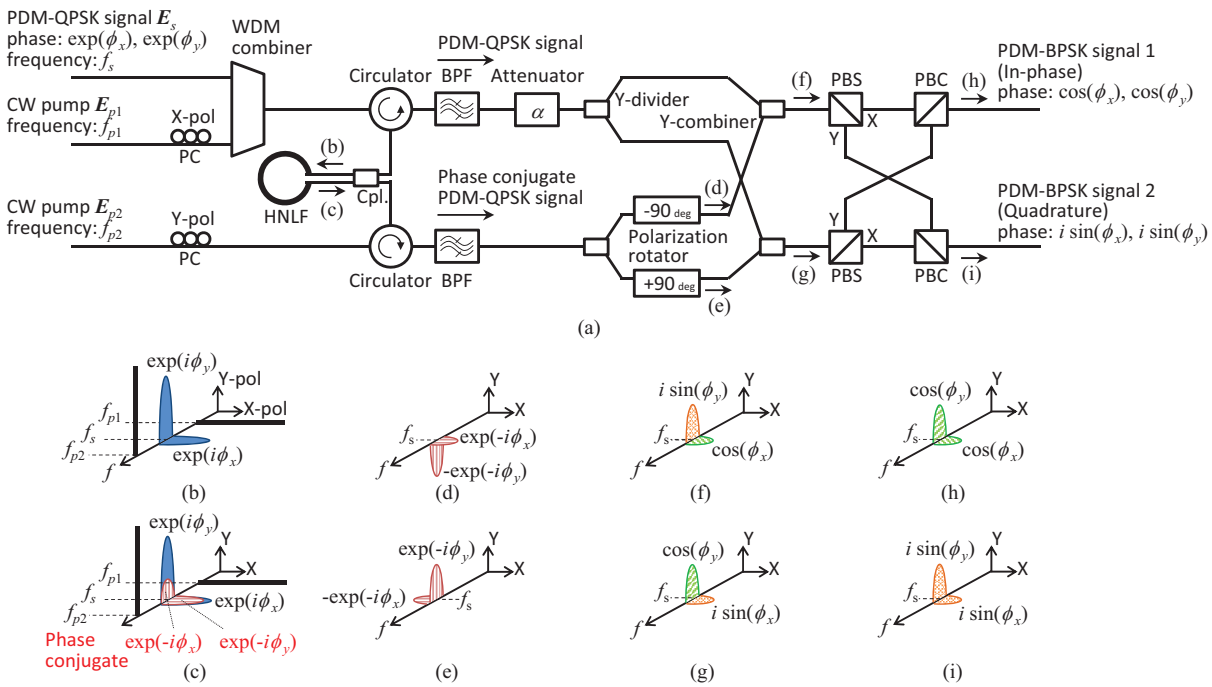

Fig. 1. Schematic diagram of the proposed all-optical wavelength preserved modulation format conversion from PDM-QPSK to PDM-BPSK, (a) system configuration and (b)-(f) signal spectra at each point indicated in (a).

These phase conjugate signals are then superimposed with the attenuated and divided original signals at Y-combiners in order to obtain converted BPSK signals. At the output of the upper side Y-combiner, it is shown in Fig. 1(f) as

$$\begin{aligned}\begin{pmatrix} E_{(\mathrm{f})x} \\ E_{(\mathrm{f})y} \end{pmatrix} =& \frac{1}{2}\begin{pmatrix} \alpha E_x \exp(i\phi_x(t)) \\ \alpha E_y \exp(i(\phi_y(t)+\theta)) \end{pmatrix} + \\ & \frac{1}{2}\begin{pmatrix} \alpha E_x \exp(-i\phi_x(t)) \\ -\alpha E_y \exp(-i(\phi_y(t)+\theta)) \end{pmatrix} \\ =& \begin{pmatrix} \alpha E_x \cos(\phi_x(t)) \\ \alpha E_y i \sin(\phi_y(t)+\theta) \end{pmatrix}. \end{aligned} \tag{6}$$

Similarly, at the output of the lower side Y-combiner, it is shown in Fig. 1(g) as

$$\begin{aligned}\begin{pmatrix} E_{(\mathrm{g})x} \\ E_{(\mathrm{g})y} \end{pmatrix} =& \frac{1}{2}\begin{pmatrix} \alpha E_x \exp(i\phi_x(t)) \\ \alpha E_y \exp(i(\phi_y(t)+\theta)) \end{pmatrix} + \\ & \frac{1}{2}\begin{pmatrix} -\alpha E_x \exp(-i\phi_x(t)) \\ \alpha E_y \exp(-i(\phi_y(t)+\theta)) \end{pmatrix} \\ =& \begin{pmatrix} \alpha E_x i \sin(\phi_x(t)) \\ \alpha E_y \cos(\phi_y(t)+\theta) \end{pmatrix}. \end{aligned} \tag{7}$$

$E_{(\mathrm{f})y}$ and $E_{(\mathrm{g})y}$ are exchanged by using PBSs and PBCs to reconstruct in-phase BPSK and quadrature BPSK signals at both polarizations. The in-phase component is shown in Fig. 1(h) as

$$\begin{pmatrix} E_{(\mathrm{in-phase})x} \\ E_{(\mathrm{in-phase})y} \end{pmatrix} = \begin{pmatrix} \alpha E_x \cos(\phi_x(t)) \\ \alpha E_y \cos(\phi_y(t)+\theta) \end{pmatrix} \tag{8}$$

and the quadrature component is shown in Fig. 1(i) as

$$\begin{pmatrix} E_{(\mathrm{quadrature})x} \\ E_{(\mathrm{quadrature})y} \end{pmatrix} = \begin{pmatrix} \alpha E_x i \sin(\phi_x(t)) \\ \alpha E_y i \sin(\phi_y(t)+\theta) \end{pmatrix}. \tag{9}$$

The phase difference θ between x- and y-polarization components should be zero or integer multiples of π, i.e. $\theta = \pm m\pi$ $(m = 0, 1, 2, \ldots)$ so that the converted signal keeps the BPSK phase.

When the original QPSK signal has a certain rotation angle ψ to the x-axis on the x-y polarization plane, (1) is modified as

$$\begin{aligned}&\begin{pmatrix} E'_{sx} \\ E'_{sy} \end{pmatrix} \\ &= \begin{pmatrix} \cos\psi & -\sin\psi \\ \sin\psi & \cos\psi \end{pmatrix}\begin{pmatrix} E_x \exp(i\phi_x(t)) \\ E_y \exp(i\phi_y(t)) \end{pmatrix} \\ &= \begin{pmatrix} E_x \cos\psi \exp(i\phi_x(t)) - E_y \sin\psi \exp(i\phi_y(t)) \\ E_x \sin\psi \exp(i\phi_x(t)) + E_y \cos\psi \exp(i\phi_y(t)) \end{pmatrix} \end{aligned} \tag{10}$$

where $\theta = 0$ is assumed. Applying similar manners from (2) to (9), the output in-phase and quadrature components become

$$\begin{aligned}&\begin{pmatrix} E'_{(\mathrm{in-phase})x} \\ E'_{(\mathrm{in-phase})y} \end{pmatrix} \\ &= \begin{pmatrix} \alpha E_x \cos\psi \cos(\phi_x(t)) - \alpha E_y \sin\psi \cos(\phi_y(t)) \\ \alpha E_x \sin\psi \cos(\phi_x(t)) + \alpha E_y \cos\psi \cos(\phi_y(t)) \end{pmatrix} \\ &= \begin{pmatrix} \cos\psi & -\sin\psi \\ \sin\psi & \cos\psi \end{pmatrix}\begin{pmatrix} \alpha E_x \cos(\phi_x(t)) \\ \alpha E_y \cos(\phi_y(t)) \end{pmatrix} \end{aligned} \tag{11}$$

and

$$\begin{aligned}&\begin{pmatrix} E'_{(\mathrm{quadrature})x} \\ E'_{(\mathrm{quadrature})y} \end{pmatrix} \\ &= \begin{pmatrix} \alpha E_x \cos\psi \cdot i\sin(\phi_x(t)) - \alpha E_y \sin\psi \cdot i\sin(\phi_y(t)) \\ \alpha E_x \sin\psi \cdot i\sin(\phi_x(t)) + \alpha E_y \cos\psi \cdot i\sin(\phi_y(t)) \end{pmatrix} \\ &= \begin{pmatrix} \cos\psi & -\sin\psi \\ \sin\psi & \cos\psi \end{pmatrix}\begin{pmatrix} \alpha E_x i \sin(\phi_x(t)) \\ \alpha E_y i \sin(\phi_y(t)) \end{pmatrix}, \end{aligned} \tag{12}$$

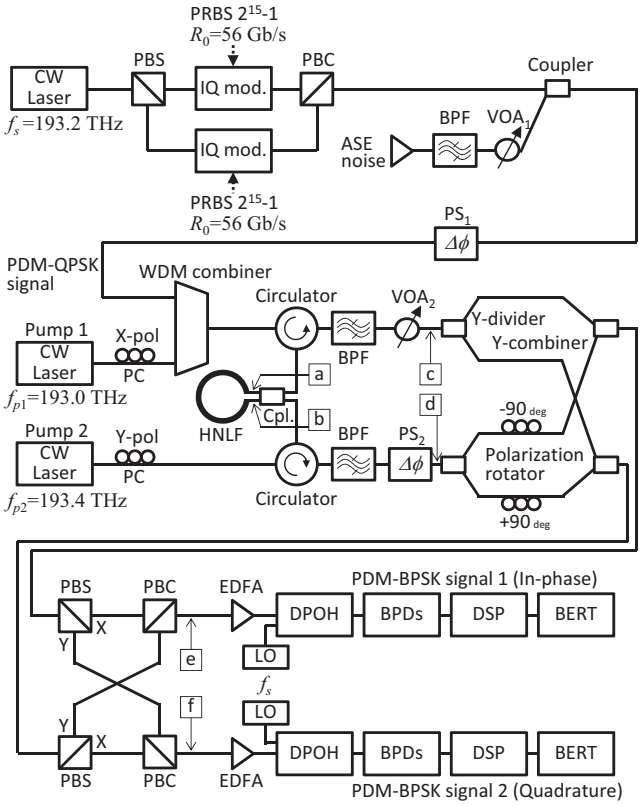

Fig. 2. Setup used in numerical simulation.

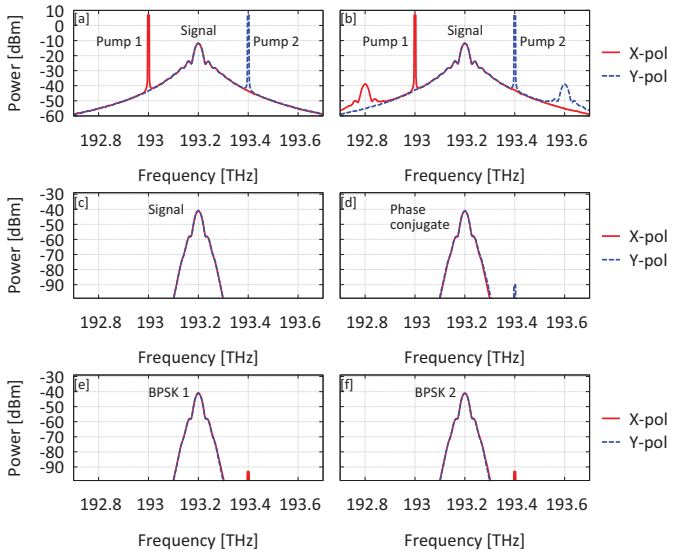

Fig. 3. Optical spectra with 0.05 nm resolution at each point (a)-(f) shown in Fig. 2.

respectively. As a result, the polarization rotation angle ψ does not matter because it is transferred to the output as it is. Therefore, this method can be applied to arbitrary angles of ψ for PDM-QPSK signals.

Consider when the original signal is assumed to propagate in a retardation plate whose Jones matrix has complex elements, a relative phase difference between each polarization component is imposed on the signal. As a result, the converted signal becomes no longer the PDM-BPSK signal.

III. Numerical Simulation

The proposed format conversion method for PDM signal is verified by numerical simulation using OptiSystem (Optiwave Systems Inc.). The system setup is shown in Fig. 2. The original 112 Gbit/s non-return-to-zero (NRZ) PDM-QPSK signal at 28 Gbaud is generated by using a 16-dBm laser source at $f_s = 193.2$ THz with 0.1-MHz linewidth, a PBS/PBC, and IQ modulators with $2^{15} - 1$ pseudorandom binary sequence (PRBS) at bit rate of $R_0 = 56$ Gb/s for each polarization component. Two CW pump laser sources are at $f_{p1} = 193.0$ THz and $f_{p2} = 193.4$ THz with 0.1-MHz linewidths and no added noise. The CW laser sources for signal and pumps are assumed to be phase-locked so that the phase matching condition between them is maintained. The free-running local oscillators (LOs) for coherent detection have power of 10 dBm at f_s with 0.1-MHz linewidths. Amplified spontaneous emission (ASE) noise is added to both polarization components of the original PDM-QPSK signal to measure bit-error-rate (BER) performance. The phase shifter (PS_1) is used to adjust the initial phase of the incident QPSK signal after the modulation to have the same initial phase as the two pumps which is set to zero in the simulation. The WDM combiner has bandwidth of 112 GHz. The 3-dB coupler has $50:50$ coupling ratio. The HNLF has nonlinearity of $n_2 = 2.7\times10^{-20}$ m^2/W and effective area of $A_{\text{eff}} = 1.5$ μm^2 [22], length of $L = 100$ m, and zero-dispersion wavelength at f_s with its slope of zero. Note that the effective area is an order of magnitude small than typical HNLF since we need to obtain sufficient phase conjugate signal power even in a relatively weak pump power around 10 dBm compared to other studies. The reason of the weak pump power is that we plan to compare results obtained by using HNLF and SOA in the future as in [18]. We use the split-step Fourier method to calculate the HNLF propagation. Circulators are assumed to have no insertion loss. Each BPF after the circulator has a Gaussian-shape transmission function with no insertion loss and bandwidth of 56 GHz centered at f_s. The variable optical attenuator (VOA_2) adjusts the intensity of the original signal to the same value as that of the phase conjugate signal. We set the VOA_2 to 26.2 dB, 32.2 dB, and 38.2 dB when pump powers are at 13 dBm, 10 dBm, and 7dBm, respectively. The phase shifter (PS_2) adjusts the phase of the phase conjugate signal in order to compensate for a relative phase deviation caused by path length difference. The phase conjugate signal is divided into two streams and they are polarization rotated at $+90$ and -90 degrees, then superimposed with the original signals at Y-combiners to be converted to two BPSK signals. The insertion loss of the Y-dividers and the Y-combiners is 3 dB, while the polarization rotators have no insertion loss. Using following PBSs and PBCs, y-polarization components of the two BPSK signals are exchanged to reconstruct in-phase BPSK and quadrature BPSK signals for both polarizations. These PBSs and PBCs are assumed to have ideal isolation and no insertion loss. Although most of the above passive components except for the HNLF have ideal properties, degradations expected on the

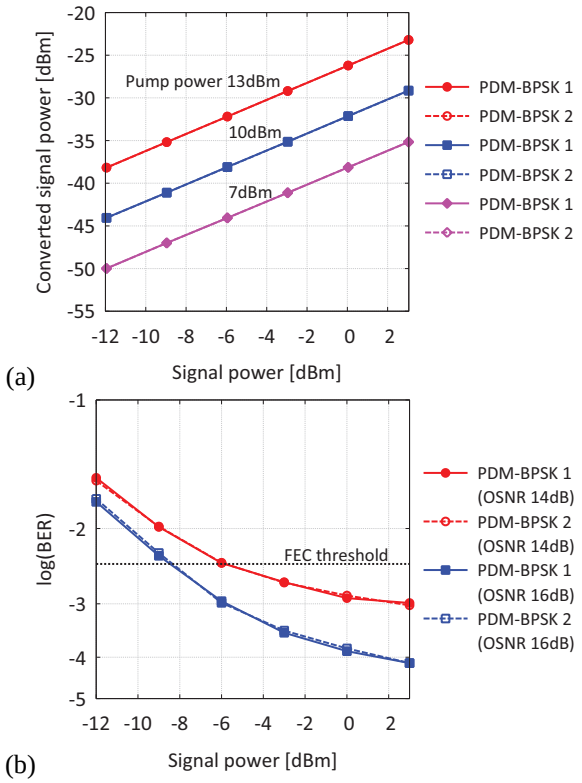

Fig. 4. Simulated results showing (a) converted PDM-BPSK signal power as a function of original PDM-QPSK signal power with pump power as a parameter and (b) BER as a function of original PDM-QPSK signal power with OSNR as a parameter.

converted signal in a real implementation are additional loss, phase rotation due to intensity imbalance and phase mismatch in between the original signal and the phase conjugate signal, and crosstalk due to the imperfect isolation in the polarization exchange by PBCs and PBSs. The two PDM-BPSK signals are amplified by the EDFAs with 36.5-dB gain and noise figure of 4 dB and coherently detected by using dual-polarization optical hybrids (DPOHs) and balanced photo detectors (BPDs) and digitally processed by adaptive equalization [23], frequency offset estimation [24] and carrier phase estimation [25] in digital signal processor (DSP). Then, bit errors are directly counted by bit error rate tester (BERT).

Fig. 3 shows optical spectra with 0.05 nm resolution at each point from (a) to (f) shown in Fig. 2. Solid and dashed curves indicate signals or pumps on x- and y-polarization, respectively. In this figure, the ASE noise is added to set the original PDM-QPSK signal's OSNR to 16 dB. Note that the CW pumps are slightly remained at outer side of the signal in Figs. 3(d)-(f) due to the finite sideband suppression of the BPFs after the circulators, which will not affect the received signal quality since they are further suppressed by the receiver's bandwidth limitation assumed to be 0.75 times of the symbol rate with the form of Bessel function.

Fig. 4(a) shows the converted PDM-BPSK signal power as a function of the original PDM-QPSK signal power with the two pumps power of 13 dBm, 10 dBm, and 7 dBm as a parameter. The original and the converted signal power are measured at the input of the WDM combiner and at the output of the PBC, respectively. The original PDM-QPSK signal is assumed to have x and y components aligned to the polarization of the pump 1 and 2, respectively. Each curve takes average values between both polarization components. The OSNR of the original signal is set to 16 dB. It is found that the converted signal power is proportional to the original signal power and the two pumps power. When the original signal power of 0 dBm and the two pumps power of 10 dBm, the converted signal power is -32.2 dBm. The conversion efficiency defined as the ratio of the converted signal power to the original signal power becomes -26.2 dB, -32.2 dB, and -38.2 dB at the pump power of 13 dBm, 10 dBm, and 7 dBm, respectively. Note that the OSNR of the signal is not degraded through conversion process itself regardless of its efficiency since the ASE noise added in advance is dominant and the quantum noise is not added from the WDM combiner to the PBCs in the simulation. Moreover, noise accumulation due to the pump-to-idler phase noise transfer in the FWM process [26] does not occur in our simulation because the signal and the two pumps are assumed to be phase-locked. It also holds in experimental verifications [27].

Fig. 4(b) shows the BER performance of the converted PDM-BPSK signals as a function of power of the original PDM-QPSK signal with its OSNR of 14 dB and 16 dB as a parameter. The signal power and the OSNR are measured before entering the WDM combiner and power of the two CW pumps is set to 10 dBm. Each curve takes average BER values between both polarization components. It is found that higher OSNR shows better BER performance and there are certain noise floors at higher signal power, which can be explained qualitatively by the ASE noise accumulated in the EDFA. We used a noise model for the EDFA as reported in [28, (23)], which can be rewritten as

$$S_{\mathrm{out}}(\lambda_s) = Gh\nu\left(10^{NF[\mathrm{dB}]/10} - \frac{1}{G} + \frac{S_{\mathrm{in}}(\lambda_s)}{h\nu}\right) \qquad (13)$$

where $S_{\mathrm{out}}(\lambda_s)$ and $S_{\mathrm{in}}(\lambda_s)$ are the output and the input ASE spectral density [W/Hz] at the signal wavelength, respectively, G is the amplifier gain, $h\nu$ is the photon energy, and NF is the noise figure of the EDFA. The first term in the parentheses is the spontaneous emission noise generated in the EDFA, the second term is the shot noise, and the third term corresponds to the noise existed in the signal before entering the EDFA. The second term is negligible in high G as 36.5 dB in the simulation compared to other terms. Therefore, curves in Fig. 4(b) can be explained by the magnitude relation between the first and the third terms. Let us consider that the range of the converted PDM-BPSK signal power entering the EDFA is from -44 to -29 dBm as shown in the curve of 10-dBm pump power in Fig. 4(a). Then, the third term is dominant when the converted signal power is relatively strong and its ONSR is assumed to be up to 16 dB which we set for the original signal. Therefore, the BER curves in Fig. 4(b) show floors since the output OSNR suffers only a slight degradation by the weak first term. Whereas both terms are comparable when the power is relatively weak, which leads to add the spontaneous emission noise amplified in the EDFA to the

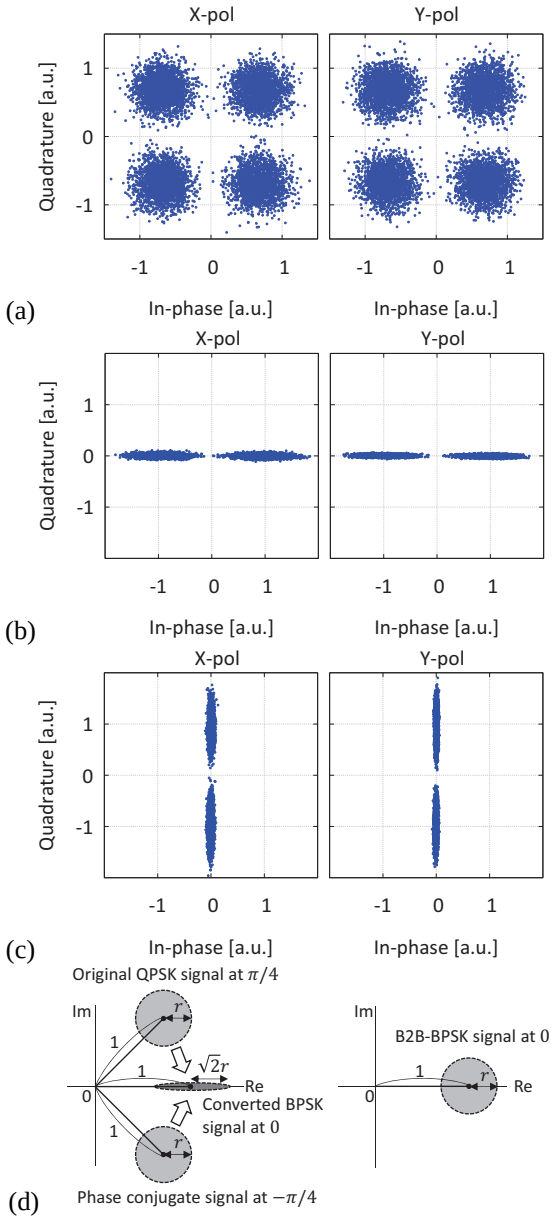

Fig. 5. Constellation map of (a) the original PDM-QPSK signal and the converted (b) in-phase and (c) quadrature PDM-BPSK signals, and (d) schematic of the phase-to-amplitude noise conversion.

already existed noise in the signal. Thus, the output OSNR is degraded significantly, which results in degradation of BER. When the OSNR of the converted signal is assumed to be sufficiently high, for instance, over 30 dB, the first term is dominant and thus the output OSNR is significantly degraded from the input OSNR. Note that included noise sources for the photo detectors are LO-ASE beat noise, signal-ASE beat noise, ASE-ASE beat noise, thermal noise, shot noise, and dark current. Due to the BPD configuration, the LO-ASE beat noise predominates over the others in the receiver [29]. In Fig. 4(b), the 7% overhead hard-decision forward error correction (FEC) threshold of $\log(3.8 \times 10^{-3}) = -2.42$ is also shown. Error-free conversion can be achieved since all curves are below the threshold at moderate signal power.

Sample constellation maps of the original PDM-QPSK signal, the converted in-phase and quadrature PDM-BPSK signals are shown in Figs. 5(a), (b) and (c), respectively. The original signal's power and OSNR are 0 dBm and 16 dB, respectively. Note that in Fig. 5 the original signal's field is normalized to have average intensity of 1. It is found that the converted signals have squeezed constellation diagrams projected onto horizontal and vertical axes due to the conversion principle, i.e. superimpose between the original and the phase conjugate signals. Fig. 5(d) illustrates the schematic of the phase-to-amplitude noise conversion compared with back-to-back (B2B)-BPSK constellation. Let us consider a case that the original QPSK signal at the constellation point of $\pi/4$ is assumed to spread as radius r by the noise added in advance of the format conversion. In this case, the phase conjugate signal generated by the FWM is to be at the constellation point of $-\pi/4$ with similar noise spread. These two signals are superimposed by a power combiner with 3-dB loss. As a result, phase-to-amplitude noise conversion occurs in the converted BPSK signal whose noise spreads as $\sqrt{2}r$ on the in-phase (real) axis. Compared to the B2B-BPSK signal with noise spread r equivalent to the original QPSK signal, the converted BPSK signal has $\sqrt{2}$-times noise spread on the in-phase axis. Therefore, the converted BPSK signal has a 3-dB OSNR penalty required for achieving the same BER as the B2B-BPSK signal by hard-decision BER calculation in which the decision threshold is on the quadrature (imaginary) axis. It is worth noting that, in terms of BER calculation, one should pay attention to the signal quality after the EDFA as described in the former paragraph. If the first term in (13) is dominant, resulting BER will have a negligible OSNR penalty compared to the B2B case. A PSA operating in gain saturation [30] is one of the candidate methods to compensate for such amplitude noise.

Fig. 6 shows the BER performance of the converted PDM-BPSK signals as a function of OSNR of the original PDM-QPSK signal with its power and pump power as parameters. In Fig. 6(a), the signal power measured before entering the WDM combiner is changed in steps of 6 dB as -12, -6 and 0 dBm, and the pump power is fixed to 10 dBm. In addition, BER performance of the original PDM-QPSK signal at power of 0 dBm is shown. As a reference, a B2B BER performance evaluated for 0-dBm PDM-BPSK signal without format conversion is also plotted, which has 0.5-dB OSNR penalty from theoretical value [31] due to additional degradations such as bandwidth limitation and noise accumulation at the receiver. At OSNR of 16 dB, the evaluated $\log$(BER) are -3.9 and -2.9 when the signal power are 0 dBm and -6 dBm, respectively, which exactly corresponds to the curve of 16-dB OSNR in Fig. 4. Moreover, the evaluated $\log$(BER) increases from -3.9 to -2.8 when the OSNR decreases from 16 dB to 14 dB at signal power of 0 dBm, which meets BER values of OSNR of 16 dB and 14 dB at that signal power in Fig. 4. It is found that there is negligible OSNR penalty in between the original PDM-QPSK signal and the converted PDM-BPSK signal at 0-dBm signal power. It is also found that almost 3-dB OSNR penalty can be observed from B2B at signal power of 0 dBm on the FEC threshold. The reason has already been

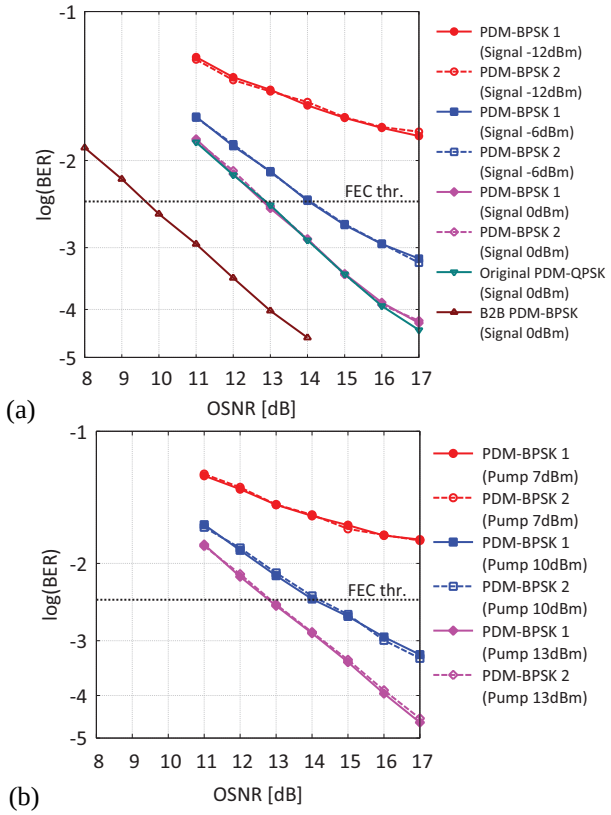

Fig. 6. BER as a function of OSNR with (a) signal power and (b) pump power as parameters.

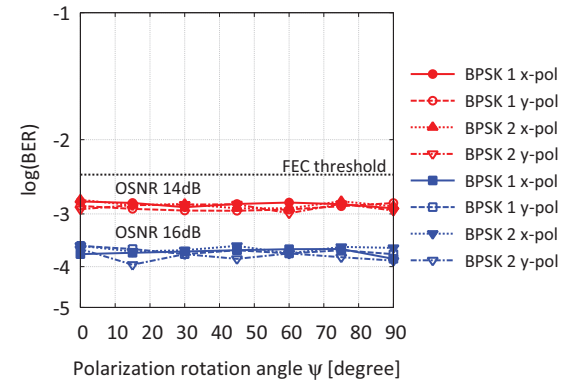

Fig. 7. BER as a function of polarization rotation angle ψ with OSNR as a parameter.

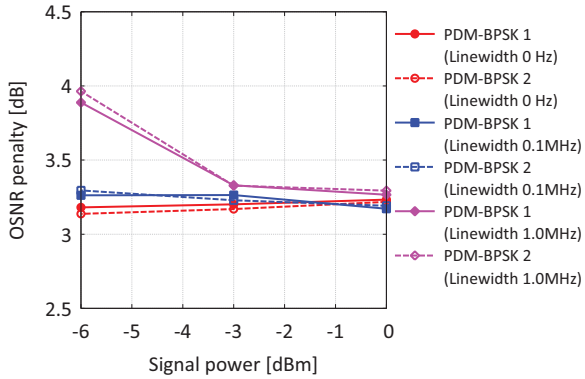

Fig. 8. OSNR penalty from B2B at BER on the FEC threshold as a function of signal power with linewidth as a parameter.

described in the explanation for Fig. 5(d). On the other hand, studies in [10], [11], [15] reported almost negligible or slight penalties from B2B results. They evaluated BER as a function of received power, not of OSNR. The ASE noise was not intentionally loaded before format conversion, but the received signal was preamplified by an EDFA. Therefore, the ASE noise generated at the EDFA was dominant both for converted signal and B2B signal, resulted in a negligible penalty except for the experimental imperfections.

In Fig. 6(b), the pump power is changed in steps of 3 dB as $+7$, $+10$ and $+13$ dBm, and the signal power is fixed to -6 dBm. As can be seen in Figs. 6(a) and (b) that they have almost the same curves except for the B2B curve. This is due to the fact that with respect to the intensity of the phase conjugate signal derived as (3), 3-dB pump power change is equivalent to 6-dB signal power change. Therefore, BER curves at signal power of -12, -6 and 0 dBm in Fig. 6(a) correspond to those at pump power of $+7$, $+10$ and $+13$ dBm in Fig. 6(b), respectively.

Fig. 7 shows the BER performance of the converted PDM-BPSK signals as a function of the polarization rotation angle of the original PDM-QPSK signal with its OSNR of 14 dB and 16 dB as a parameter. At $\psi = 0$, x- and y-polarization components are along with pump 1 and pump 2, respectively. The signal power and the pump power are set to 0 dBm and 10 dBm, respectively. It is found that there is no dependency on BER to ψ of the original signal. Therefore, it is confirmed that this method can be used for arbitrary angles of ψ for PDM-QPSK signals.

Fig. 8 shows the OSNR penalty, which is the difference of the OSNR required for BER on the FEC threshold between the converted PDM-BPSK signal and the respective B2B result, as a function of the original PDM-QPSK signal power with linewidth of the signal and the pump laser sources as a parameter. The pump power is set to 10 dBm. At 0-dBm signal power, almost 3-dB OSNR penalty is observed at any linewidths of 0, 0.1, 1.0 MHz. When the signal power decreases, the OSNR penalty increases with the linewidth. This is because broader pump bandwidth, especially the bottom of the spectrum, is overlapped with the signal bandwidth and thereby causes crosstalk. For instance, the crosstalk on the phase conjugate signal at 1.0-MHz linewidth and -6-dBm signal power is comparable to the (inverse of) required OSNR for the target BER, which results in signal quality degradation. The crosstalk is almost 10-dB weaker at 0.1-MHz linewidth and -6-dBm signal power.

IV. Discussion

This section discusses some important issues for practical use of the proposed conversion scheme. First, we consider the phase difference of θ between each polarization component expressed as (1). This phase difference θ is included within cosine and sine functions of the y-polarization component

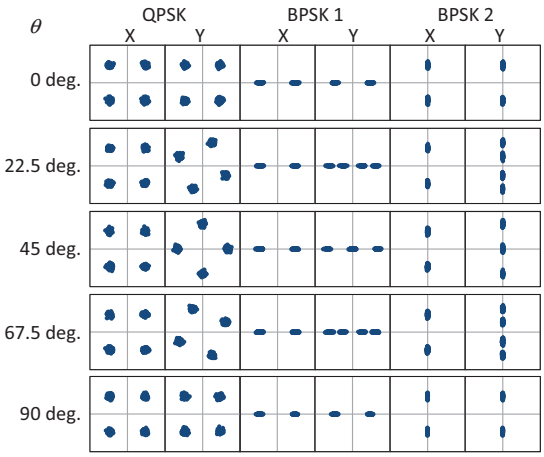

Fig. 9. Constellation diagrams of the original QPSK signal and the converted two BPSK signals at $\theta = 0$, 22.5, 45, 67.5 and 90 degrees.

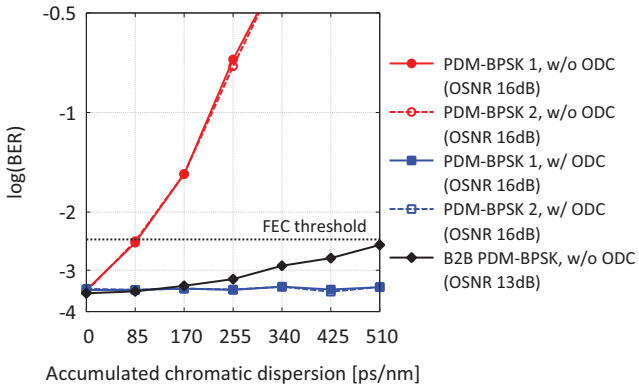

Fig. 10. BER as a function of chromatic dispersion accumulated before format conversion.

of the converted BPSK signals expressed as (8) and (9). It means that taking cosine and sine after rotating the original QPSK signals by θ becomes no longer the correct in-phase and quadrature components projected onto horizontal and vertical axes. Fig. 9 shows constellation diagrams of the original QPSK signal and the converted two BPSK signals at $\theta = 0$, 22.5, 45, 67.5 and 90 degrees. The OSNR of the original QPSK signal is set to 26 dB. It is found that y-polarization of the converted in-phase BPSK 1 and the quadrature BPSK 2 at $\theta = 22.5$, 45 and 67.5 degrees have four, three and four constellation points, respectively, not corresponding to BPSK phases. At $\theta = 90$ degree, they look like the same constellation as $\theta = 0$ degree, however, the in-phase and the quadrature components are swapped which is easily calculated from (8) and (9). Consider the pump phase adjustment to compensate for θ, however, it will not work since it is equally included outside of cosine and sine functions of both polarizations in (8) and (9). Moreover, in experimental verifications, the relative phase between both polarization channels will vary in time unless an integrated PDM-modulator [32] is used. Further investigations on how to deal with such time-variant and invariant phase are our future works.

Next, we consider undergone transmission impairments

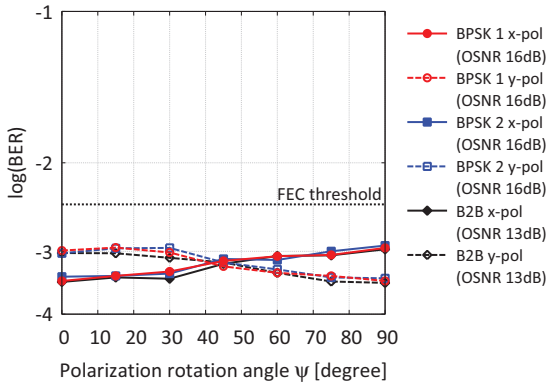

Fig. 11. BER as a function of polarization rotation angle ψ with 3-dB PDL on the vertical axis.

before format conversion such as chromatic dispersion (CD), polarization dependent loss (PDL), polarization mode dispersion (PMD), and nonlinear effects. They normally degrade a signal simultaneously, though, we evaluate them independently and nonlinear effects are ignored for simplicity. Consider CD accumulated before format conversion, the incident signal's amplitude and phase are degraded. As expressed in (8) and (9), the amplitude goes out as it is through the system, however, the phase are included in sine and cosine function. Therefore, conventional post-processing dispersion compensation (DC) methods such as optical DC (ODC) and frequency domain electrical DC (EDC) at the receiver may not compensate for the accumulated CD even when using known information about transmission channel, for instance, fiber length, dispersion coefficient, and etc. A simple solution is to apply ODC before format conversion. Fig. 10 shows the BER performance of the converted PDM-BPSK signals as a function of CD accumulated before format conversion. In the simulation, a CD emulator is placed before the WDM combiner, assuming the dispersion coefficient of 17 ps/nm/km and the dispersion slope of 0.075 ps/nm^2/km at f_s without fiber loss. Accumulated CD is emulated by changing its fiber length from 0 km to 30 km. The signal and the pump powers are set to -3 dBm and 10 dBm, respectively. It is found that BER exceeds the FEC threshold over 85-ps/nm CD which corresponds to 5-km fiber length without the use of ODC, whereas it keeps below the FEC threshold with ODC placed between the CD emulator and the WDM combiner. In the B2B case in which no format conversion is performed and a CD emulator is placed before the receiver, a 13-dB OSNR B2B curve shows a gradual BER increase despite no ODC. This is because the 13-tap adaptive equalizer in the receiver DSP partly compensates for the accumulated CD. The reason why the 13-dB OSNR B2B curve, 3-dB less than the original signal, is plotted is that the converted signal has 3-dB OSNR penalty compared to the B2B case to achieve the same BER as explained in Fig. 5(d). Note that if the converted in-phase and quadrature PDM-BPSK signals are allowed to be received at the same time and transformed into a complex exponential signal using Euler's formula, the accumulated CD can be compensated by the conventional EDC.

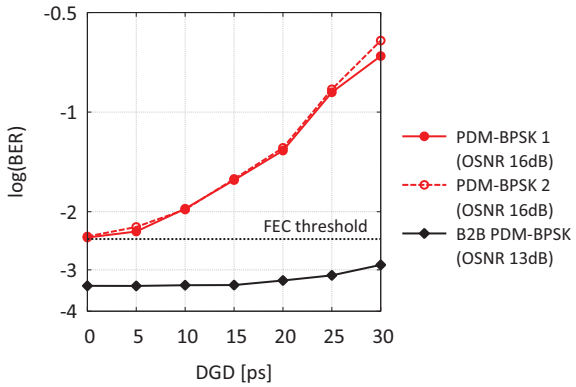

Fig. 12. BER as a function of DGD with emulated PMD effects on the original PDM signal.

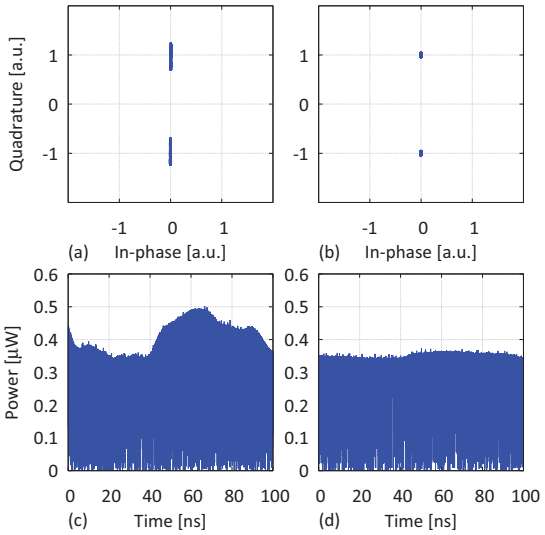

Fig. 13. Examples of (a)(b) constellations and (c)(d) waveforms of the converted quadrature BPSK signal on x-polarization when phase-locking between signal and pumps is (b)(d) activated and (a)(c) not activated.

Then, we evaluate the influence of PDL on the original PDM signal. As described in [33], the system PDL shows statistical nature in point-to-point transmission system because there is a number of optical devices with constant PDL in network nodes connected by a transmission fiber in which the state of polarization (SOP) can be randomly converted. However, we conduct a deterministic calculation to evaluate two impairments by PDL, namely, the level imbalance and the loss of orthogonality. The former corresponds to power loss on the lossy polarization axis and the latter corresponds to crosstalk on both polarization axes [34]. In the simulation, the signal and the pump powers are set to -3 dBm and 10 dBm, respectively. A PDL element with 3-dB loss only on the vertical axis is placed before the WDM combiner. Fig. 11 shows the BER performance of the converted PDM-BPSK signals as a function of the polarization rotation angle ψ of the original PDM-QPSK signal with its OSNR of 16 dB. It is found that all results are below the FEC threshold. At $\psi = 0$ degree, only y-polarization component shows worse BER which exactly corresponds to -6-dBm signal power in Fig. 4. When ψ increases, x-pol and y-pol curves are crossed at 45 degree at which both polarization components show the same BER due to the same loss on the vertical axis, and then separated again up to 90 degree at which originally x-polarization component shows worse BER. As explained in Fig. 5(d) about the 3-dB OSNR penalty, B2B results with OSNR of 13 dB plotted in Fig. 11 also show the similar curves. Therefore, it is confirmed that the conversion method does not suffer additional performance degradation by the deterministic PDL.

Consider PMD, as reported in [35], it also shows statistical nature since the single-mode fiber contains arbitrary birefringence varying in time and in length due to random imperfections and asymmetries such as stress, heat and vibration. It may cause delay and superposition between two polarization components, pulse deformation and related phase change. In this discussion, we conduct a deterministic calculation to evaluate combined impairments by PMD, namely, frequency independent differential group delay (DGD), frequency dependence of DGD and the principle states of polarization (PSP) as described in [36]. In the simulation, the signal and the pump powers are set to -3 dBm and 10 dBm, respectively. A PMD emulator is placed before the WDM combiner, assuming that emulated fiber length is 50 km, negligible chromatic dispersion and slope, frequency dependence of DGD called polarization chromatic dispersion is 1.3 ps/GHz, and frequency dependence of the PSP referred to as depolarization rate is 10.8 deg/GHz [36]. Fig. 12 shows the BER performance of the converted PDM-BPSK signals as a function of the value of DGD with OSNR of 16 dB. It is found that the BER exceeds the FEC threshold and becomes monotonically worse with DGD. In the B2B case in which a PMD emulator is placed before the receiver, a 13-dB OSNR B2B curve shows a slight BER increase but below the FEC threshold. This is because the adaptive equalizer in the receiver DSP aggressively compensates for the PMD effects in the B2B case, whereas the format conversion is strongly affected by the PMD-induced phase change even when the receiver DSP is activated. Further investigation to suppress such PMD effects on the PDM signals is our another future work.

Finally, we discuss on how to achieve the phase-locking between signal and pump laser sources. In the proposed method, dynamic adjustment is needed for the phase-locking and to guarantee the state of polarization of the incident PDM-QPSK signal as $\theta = \pm m\pi$ $(m = 0, 1, 2, \ldots)$ as already described. Note that when the pump power is constant, values of PS_1, PS_2, and VOA_2 in Fig. 2 can be fixed after they have been once optimized. They don't depend on the original signal intensity. In order to stabilize the phase fluctuation, a feedback loop architecture is usually employed. For instance as reported in [13], the output of an optical phase comparator has been used as the error signal in a phase-locked loop. Another possible phase-locking method reported in [17] utilizes a multiply-filter-divide technique. A frequency comb source with a single common laser can also be used to lock the phase between two pumps needed for our method. Note that even when the frequency comb source is used not only for the two pumps

but also for the signal, phase stabilization is necessary since the signal is modulated whereas the pumps are not modulated. Fig. 13 shows constellations and waveforms of the converted quadrature BPSK signal on x-polarization measured after the PBS when the phase-locking method in [17] between signal and pumps is implemented or not. In the simulation, 1-MHz linewidth is set to the CW laser for the original signal. No ASE noise is added to the original signal. Two pumps are assumed to have zero linewidth. Therefore, only the signal phase is adjusted by the phase-locking method shown in [17, Fig. 2] which generates a feedback signal by using a photo detector, a radio frequency (RF) amplifier, a RF detector, analog-to-digital converter, and a DSP. As shown in Fig. 13, the amplitude fluctuation caused by the phase drift is clearly reduced by using the phase-locking method. Note that the amplitude fluctuation will change in each calculation iteration because such phase drift normally shows stochastic nature.

The other aspect of the phase-locking in our system is the stabilization of the interference at Y-combiners between the original signal and the phase conjugate signal they have propagated along different paths. Consider a case where a relative phase difference of -2δ is remained to the phase conjugate signal expressed as (4) and (5) compared to the original signal, the converted BPSK signals after the Y-combiners expressed as (6) and (7) are modified as

$$\begin{aligned}\begin{pmatrix} E'_{(\mathrm{f})x} \\ E'_{(\mathrm{f})y} \end{pmatrix} =& \frac{1}{2}\begin{pmatrix} \alpha E_x \exp(i\phi_x(t)) \\ \alpha E_y \exp(i\phi_y(t)) \end{pmatrix} + \\ & \frac{1}{2}\begin{pmatrix} \alpha E_x \exp(-i\phi_x(t))\exp(-i2\delta) \\ -\alpha E_y \exp(-i\phi_y(t))\exp(-i2\delta) \end{pmatrix} \\ =& \begin{pmatrix} \alpha E_x \cos(\phi_x(t)+\delta)\exp(-i\delta) \\ \alpha E_y i \sin(\phi_y(t)+\delta)\exp(-i\delta) \end{pmatrix} \end{aligned} \quad (14)$$

and

$$\begin{aligned}\begin{pmatrix} E'_{(\mathrm{g})x} \\ E'_{(\mathrm{g})y} \end{pmatrix} =& \frac{1}{2}\begin{pmatrix} \alpha E_x \exp(i\phi_x(t)) \\ \alpha E_y \exp(i\phi_y(t)) \end{pmatrix} + \\ & \frac{1}{2}\begin{pmatrix} -\alpha E_x \exp(-i\phi_x(t))\exp(-i2\delta) \\ \alpha E_y \exp(-i\phi_y(t))\exp(-i2\delta) \end{pmatrix} \\ =& \begin{pmatrix} \alpha E_x i \sin(\phi_x(t)+\delta)\exp(-i\delta) \\ \alpha E_y \cos(\phi_y(t)+\delta)\exp(-i\delta) \end{pmatrix}, \end{aligned} \quad (15)$$

respectively, where $\theta = 0$ is assumed. As a result, δ included in the sine and cosine functions will affect on both polarization components as well as θ in the original equations and shown in Fig. 9. The term $\exp(-i\delta)$ corresponds to a phase shift applied after the conversion. A possible solution to stabilize the interference is the photonic integrated circuit. Although simulations are performed with a HNLF, any nonlinear media supporting the possibility of integration can be used such as SOA and silicon nanowires. By using such media, integration of the processing system is possible. The reason why we used the HNLF in the simulation is to avoid considering parameters such as pattern effect, additional noise generation, and conversion efficiency dependence by signal-pump frequency separation when using the SOA.

V. CONCLUSION

In this paper, we have proposed an all-optical modulation format conversion system from a PDM-QPSK signal to two PDM-BPSK signals. Based on the principle of the orthogonal dual-pump FWM in NOLM and the coherent superposition, the proposed system can be applied to polarization multiplexed signals. In addition, the system has advantages of wavelength preserved conversion without any loss of data of the incident signal.

We have evaluated the system performance by numerical simulations. BER performances are affected not only by the signal power but also the pump power due to the conversion efficiency, whereas independent of the polarization rotation angle of the original signal. OSNR penalty from B2B shows almost 3 dB because of the phase-to-amplitude noise conversion caused by the operation principle.

Since the proposed system is limited to incident signals with $\theta = \pm m\pi$ $(m = 0, 1, 2, \ldots)$ as discussed in section 4, we will develop advanced methods to treat signals with arbitrary θ. Moreover, taking the phase-locking mechanism in to account, suppressing technique for PMD effects and experimental verification are also other issues to be investigated as our future works.

REFERENCES

[1] P. J. Winzer, "High-spectral-efficiency optical modulation formats," *J. Lightwave Technol.*, vol. 30, no. 24, pp. 3824–3835, Dec. 2012.
[2] A. E. Willner, S. Khaleghi, M. R. Chitgarha, and O. F. Yilmaz, "All-optical signal processing," *J. Lightwave Technol.*, vol. 32, no. 4, pp. 660–680, Feb. 2014.
[3] K. Mishina, S. Kitagawa, and A. Maruta, "All-optical modulation format conversion from on-off-keying to multiple-level phase-shift-keying based on nonlinearity in optical fiber," *Opt. Exp.*, vol. 15, no. 13, pp. 8444–8453, June 2007.
[4] K. Mishina, A. Maruta, S. Mitani, T. Miyahara, K. Ishida, K. Shimizu, T. Hatta, K. Motoshima, and K. Kitayama, "NRZ-OOK-to-RZ-BPSK modulation-format conversion using SOA-MZI wavelength converter," *J. Lightwave Technol.*, vol. 24, no. 10, pp. 3751–3758, Oct. 2006.
[5] H. Kishikawa, P. Seddighian, N. Goto, S. Yanagiya, and L. R. Chen, "All-optical modulation format conversion from binary to quadrature phase-shift keying using delay line interferometer," in *Proc. IEEE Photonics Conference (IPC2011)*, Arlington, Virginia, USA, no. WO2, pp. 513–514, Oct. 2011.
[6] F. Parmigiani, L. Jones, J. Kakande, P. Petropoulos, and D. J. Richardson, "Modulation format conversion employing coherent optical superposition," *Opt. Exp.*, vol. 20, no. 26, pp. B322–B330, Dec. 2012.
[7] R. P. Webb, J. M. Dailey, R. J. Manning and A. D. Ellis, "Phase discrimination and simultaneous frequency conversion of the orthogonal components of an optical signal by four-wave mixing in an SOA," *Opt. Exp.*, vol.19, no.21, pp.20015–20022, Oct. 2011.
[8] G. -W. Lu, E. Tipsuwannakul, T. Miyazaki, C. Lundström, M. Karlsson, P. A. Andrekson, "Format conversion of optical multilevel signals using FWM-based optical phase erasure," *J. Lightwave Technol.*, vol. 29, no. 16, pp. 2460–2466, Aug. 2011.
[9] R. P. Webb, M. Power, and R. J. Manning, "Phase-sensitive frequency conversion of quadrature modulated signals," *Opt. Exp.*, vol.21, no.10, pp.12713-12727, May 2013.
[10] F. D. Ros, K. Dalgaard, L. Lei, J. Xu, and C. Peucheret, "QPSK-to-2×BPSK wavelength and modulation format conversion through phase-sensitive four-wave mixing in a highly nonlinear optical fiber," *Opt. Exp.*, vol. 21, no. 23, pp. 28743–28750, Nov. 2013.
[11] F. D. Ros, K. Dalgaard, Y. Fukuchi, J. Xu, M. Galali, and C. Peucheret, "Simultaneous QPSK-to-2x-BPSK wavelength and modulation format conversion in PPLN," *IEEE Phton. Tech. Lett.*, vol. 26, no. 12, pp. 1207–1210, Jun. 2014.

[12] Z. Bakhtiari, "Optical demultiplexing of a QPSK data channel into two BPSK sub-channels on phase-sensitive optical amplification," in *Proc. IEEE Photonics Conference (IPC2013)*, Bellevue, Washington, USA, no. TuF3.4, Sept. 2013.
[13] M. Gao, T. Kurosu, T. Inoue, and S. Namiki, "Low-penalty phase demultiplexing of QPSK signal by dualpump phase sensitive amplifiers," in *39th European Conference and Exhibition on Optical Communication (ECOC 2013)*, paper We.3.A.5, Sept. 2013.
[14] F. Parmigiani, G. Hesketh, R. Slavík, P. Horak, P. Petropoulos, and D. J. Richardson, "Polarization-assisted phase-sensitive processor," *J. Lightwave Technol.*, vol. 33, no. 6, pp. 1166–1174, Mar. 2015.
[15] N. K. Kjøller, M. Galili, K. Dalgaard, H. C. H. Mulvad, K. M. Røge, and L. K. Oxenløwe, "Quadrature decomposition by phase conjugation and projection in a polarizing beam splitter," in *40th European Conference and Exhibition on Optical Communication (ECOC 2014)*, paper P.3.8, Sept. 2014.
[16] A. Lorences-Riesgo, T. A. Eriksson, M. Mazur, P. A. Andrekson, and M. Karlsson, "Quadrature decomposition of a 20 Gbaud 16-QAM signal into 2×4-PAM signals," in *42nd European Conference and Exhibition on Optical Communication (ECOC 2016)*, paper Tu.1.E.3, Sept. 2016.
[17] A. Lorences-Riesgo, L. Liu, S. L. I. Olsson, R. Malik, A. Kumpera, C. Lundström, S. Radic, M. Karlsson, and P. A. Andrekson, "Quadrature demultiplexing using a degenerate vector parametric amplifier," *Opt. Exp.*, vol. 22, no. 24, pp. 29424–29434, Nov. 2014.
[18] R. Ando, H. Kishikawa, N. Goto, and S. Yanagiya, "Format conversion from QPSK to BPSK using wavelength-shift-free FWM and interference," in *19th OptoElectronics and Communication Conference / Australian Conference on Optical Fibre Technology (OECC/ACOFT 2014)*, no. TUPS1-8, pp. 440–441, July 2014.
[19] R. Ando, H. Kishikawa, N. Goto, S. Yanagiya, and L. R. Chen, "Performance analysis of all-optical wavelength-shift-free format conversion from QPSK to two BPSK tributaries using FWM and interference," *IEICE Trans. on Electron.*, vol. E99-C, no. 2, pp. 219–226, Feb. 2016.
[20] N. Yoshioka, R. Ando, H. Kishikawa, and N. Goto "Polarization-diversity all-optical modulation format conversion from QPSK to BPSK using FWM," in *Asia Communications and Photonics Conference 2015 (ACP2015)*, paper ASu1E.2, Nov. 2015.
[21] H. C. Lim, F. Futami and K. Kikuchi, "Polarization-independent, wavelength-shift-free optical phase conjugator using a nonlinear fiber Sagnac interferometer," *IEEE Photon. Technol. Lett.*, vol. 11, no. 5, pp.578–580, May 1999.
[22] K. S. Abedin, "Optical signal processing using fiber nonlinearity," *J. National Institute of Information and Communications Technology*, vol. 53, no. 2, pp.9–14, June 2006.
[23] D. N. Godard, "Self-recovering equalization and carrier tracking in two-dimensional data communication systems," *IEEE Trans. Commun.*, vol. 28, no. 11, pp. 1867–1875, Nov. 1980.
[24] M. Morelli and U. Mengali, "Feed forward frequency estimation for PSK: A tutorial review," *European Transactions on Telecommunications*, vol. 9, no. 2, pp. 103–116, Mar./Apr. 1988.
[25] A. J. Viterbi, and A. M. Viterbi, "Nonlinear estimation of PSK-modulated carrier phase with application to burst digital transmission," *IEEE Trans. Inf. Theory*, vol. 29, no. 4, pp. 543–551, Jul. 1983.
[26] S. P. Ó. Dúill, S. T. Naimi, A. P. Anthur, T. N. Huynh, D. Venkitesh, and L. P. Barry, "Simulations of an OSNR-limited all-optical wavelength conversion scheme," *Photon. Technol. Lett.*, vol. 25, no. 23, pp. 2311–2314, Dec. 2013.
[27] A. P. Anthur, R. T. Watts, K. Shi, J. O'Carroll, D. Venkitesh, and L. P. Barry, "Dual correlated pumping scheme for phase noise preservation in all-optical wavelength conversion," *Opt. Exp.*, vol.21, no.13, pp.15568-15579, Jun. 2013.
[28] D. M. Baney, P. Gallion, R. S. Tucker, "Theory and measurement techniques for the noise figure of optical amplifiers," *Opt. Fiber Technol.*, vol.6, no.2, pp.122–154, Apr. 2000.
[29] S. Yamashita and T. Okoshi, "Suppression of common-mode beat noise from optical amplifiers using a balanced receiver," *Elec. Lett.*, vol. 28, no. 21, pp.1970–1972, Oct. 1992.
[30] C. Lundström, B. Corcoran, M. Karlsson, and P. A. Andrekson, "Phase and amplitude characteristics of a phase-sensitive amplifier operating in gain saturation," *Opt. Exp.*, vol.20, no.19, pp.21400–21412, Sept. 2012.
[31] R. J. Essiambre, G. Kramer, P. J. Winzer, G. J. Foschini, and B. Goebel, "Capacity limits of optical fiber networks," *J. Ligthwave Technol.*, vol. 28, no. 4, pp. 662–701, Feb. 2010.
[32] S. Mino, H. Yamazaki, T. Goh, and T. Yamada, "Multilevel optical modulator utilizing PLC-$LiNbO_3$ hybrid-integration technology," *NTT Technical Review*, vol.9, no.3, pp.1–3, Mar. 2011.
[33] K. Mori, T. Kataoka, T. Kobayashi, and S. Kawai, "Statistics and performance under combined impairments induced by polarization-dependent loss in polarization-division-multiplexing digital coherent transmission," *Opt. Exp.*, vol. 19, no. 26, pp. B673–B680, Dec. 2011.
[34] Z. Wang, C. Xie, and X. Ren, "PMD and PDL impairments in polarization division multiplexing signals with direct detection," *Opt. Exp.*, vol. 17, no. 10, pp. 7993–8004, May 2009.
[35] C. D. Poole, J. H. Winters, and J. A. Nagel, "Dynamical equation for polarization dispersion," *Opt. Lett.*, vol. 16, no. 6, pp. 372–374, Mar. 1991.
[36] C. Francia, F. Bruyère, D. Penninckx, and M. Chbat, "PMD second-order effects on pulse propagation in single-mode optical fibers," *IEEE Photon. Technol. Lett.*, vol. 10, no. 12, pp. 1739–1741, Dec. 1998.

Hiroki Kishikawa (M'15) received the B.E. and M.E. degree in information and computer sciences from Toyohashi University of Technology, Toyohashi, Japan in 2004 and 2006, respectively, and the D.E. degree in optical science and technology from The University of Tokushima, Japan, in 2012. He worked at Nomura Research Institute from 2006 to 2009. He was Research Fellow of Japan Society for the Promotion of Science from 2010 to 2012. From August 2010 to January 2011, he was with McGill University, Montreal, QC, Canada, as a graduate research trainee, where he engaged in research on optical packet format conversion. From April 2012 to March 2015, he worked for Network Innovation Laboratories, NTT Corporation. On April 2015, he joined Tokushima University as an Assistant Professor.

His research interests include photonic routing, photonic switching, and photonic networking.

Dr. Kishikawa received the Yasujiro Niwa Outstanding Paper Award in 2011 and the Young Engineer Award of the Institute of Electronics, Information, and Communications Engineers (IEICE) of Japan in 2013.

Nobuo Goto (M'88) received the B.E., M.E., and D.E. degrees in electrical engineering from Nagoya University, Nagoya, Japan, in 1979, 1981, and 1984, respectively. He was a Research Associate of the Faculty of Engineering, Nagoya University, Nagoya, Japan, from 1984 to 1986. He became a Research Associate, a Lecturer and an Associate Professor at Toyohashi University of Technology, Toyohashi, Japan, in 1986, 1989, and 1993 respectively. From April 2007, he is a Professor at The University of Tokushima, Tokushima, Japan. From August 1987 to August 1988, he was with McGill University, Montreal, QC, Canada, where he engaged in research on passive and electrooptic integrated devices. From August 2001 to August 2002, he was with Multimedia University, Malaysia, as a JICA expert for JICA project of Networked Multimedia Education System.

His research interest includes integrated optical signal processing using acoustooptic effects and photonic routing systems.

Dr. Goto received the Young Engineer Award of the Institute of Electronics, Information, and Communications Engineers (IEICE) of Japan in 1984, and the Niwa Memorial Prize in 1985. He is also a member of IEICE and IEE of Japan.

Lawrence R. Chen (SM'05) received the B.Eng. degree in electrical engineering and mathematics from McGill University, Montreal, QC, Canada, in 1995 and the M.A.Sc. and Ph.D. degrees in electrical and computer engineering in 1997 and 2000, respectively. Since 2000, he has been with the Department of Electrical and Computer Engineering at McGill University.

His research interests are in optical communications, fiber and integrated optics, and microwave photonics, and in particular, active and passive devices in silicon photonics for optical and microwave signal processing.

He is Editor-in-Chief for the IEEE Photonics Newsletter and an Editor for Optics Communications.